Geoderma 445 (2024) 116879

Contents lists available at ScienceDirect

Geoderma

journal homepage: www.elsevier.com/locate/geoderma

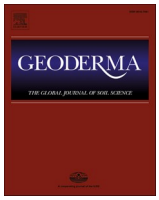

Rare earth elements in clay-sized fractions: Implications for weathering fingerprint from parent materials to soils

Xianming Zhang [a], Yuntao Jing [a,b], Wanfu Zhao [c], Yongjun Jiang [a], Dong-Xing Guan [d], Hongxia Du [e], Ying Qian [a], Fei Ye [f], Wancang Zhao [a,*]

[a] Chongqing Key Laboratory of Karst Environment & School of Geographical Sciences of Southwest University, Chongqing 400715, China
[b] School of Earth Sciences and Resources, China University of Geosciences, Beijing 100083, China
[c] Ningxia Institute of Land Resources Survey and Monitor, Yinchuan 750002, Ningxia Hui Autonomous Region, China
[d] Zhejiang Provincial Key Laboratory of Agricultural Resources and Environment, Institute of Soil and Water Resources and Environmental Science, College of Environmental and Resource Sciences, Zhejiang University, Hangzhou 310058, China
[e] College of Resources and Environment, Southwest University, Chongqing 400715, China
[f] Nanjing Institute of Environmental Sciences, Ministry of Ecology and Environment of China, Nanjing 210042, China

ARTICLE INFO

Handling Editor: A. Agnelli

Keywords:
Weathering
Clay mineralogy
Chemical analysis
Rare earths
Iron

ABSTRACT

Rare earth elements (REEs) have gained attention as tracers of pedogenic processes over the last few decades. Clay-sized fractions (CSFs, < 2 μm) may play a crucial role in hosting REEs. To better understand the pedochemical signals of REEs in clay-sized phases, such as iron oxides and phyllosilicates, we analyzed REE speciation in CSFs of carbonate rocks (limestone), clastic rocks (sandstone and shale), and their derived saprolites. Our results quantified the REE content (41.2–144.6 mg kg^{-1}) and speciation in CSFs of parent materials, revealing that REEs were primarily hosted in amorphous iron oxides (Fe_{ox1}), followed by crystalline iron oxides (Fe_{ox2}) and phyllosilicates. Compared to parent materials, saprolites derived from carbonate rocks exhibited more than a two-fold enrichment of REEs in major clay-sized phases, confirming the role of CSFs as REE sinks during carbonate rock weathering. Furthermore, the initial REE patterns of CSFs of carbonate rocks underwent alteration throughout the weathering process, likely due to water–mineral interactions. Our findings suggest that REEs in CSFs record the weathering fingerprint for soils derived from carbonate rocks, while they are indicative of provenance for soils originating from clastic rocks.

1. Introduction

Chemical weathering plays a crucial role in soil formation, driving the transportation of rare earth elements (REEs, from La to Lu) from the lithosphere to the pedosphere (Laveuf and Cornu, 2009). During weathering, REE mobility is strongly influenced by mineralogy (Braun et al., 1993; Nesbitt and Markovics, 1997; Ji et al., 2004; Laveuf and Cornu, 2009; Santos et al., 2019). The principal REE-bearing minerals include silicates, phosphates, iron oxides, and oxygenated salts (Chakhmouradian and Wall, 2012; Brioschi et al., 2013). Recently, the presence of REEs in clay-sized minerals (e.g., iron oxides and phyllosilicates) has attracted increasing attention (Laveuf et al., 2012; Denys et al., 2021; Gu et al., 2022; Liu et al., 2023). Due to the high affinity of clay-sized minerals for REEs (Koeppenkastrop and Carlo, 1993; Bau and Koschinsky, 2009; Yang et al., 2021; Liu et al., 2022), clay-sized fractions (CSFs, < 2 μm) have been considered ubiquitous carriers of REE transport and accumulation (Cullers et al., 1975; Ji et al., 2004; Bayon et al., 2015; Wu et al., 2019; Liu et al., 2023). Furthermore, given the elevated chemical reactivity of clay-sized minerals, REEs in CSFs are sensitive to weathering environment conditions (e.g., pH and redox) (Cao et al., 2001; Laveuf et al., 2012; Durn et al., 2021) and can interact with the liquid phase (Bradbury and Baeyens, 2005; Stille et al., 2009; Cidu et al., 2013; Liu et al., 2022), influencing fractionation between light REEs (LREEs) and heavy REEs (HREEs) in soil. Consequently, REE signals in CSFs could be a vital archive of regolith evolution, particularly in pedogenesis.

Current weathering models suggest that REE characteristics of bulk soils could be related to the lithology of parent material (Wei et al., 2014; Feitosa et al., 2020; Wu and Hseu, 2023). This is particularly evident in karstic areas, where bulk soils derived from carbonate rocks

* Corresponding author.
E-mail address: zhwc321@163.com (W. Zhao).

https://doi.org/10.1016/j.geoderma.2024.116879
Received 27 October 2023; Received in revised form 27 March 2024; Accepted 7 April 2024
Available online 13 April 2024

generally exhibit a several-fold enrichment of REEs relative to parent materials (Ji et al., 2004; Wei et al., 2014; Chang et al., 2019; Feitosa et al., 2020). According to previous hypotheses, this enrichment is mainly attributed to the removal of components with low REE content and, more importantly, the accumulation effect of clay-sized minerals (Ji et al., 2004). However, sedimentary rocks (e.g., carbonate and clastic rocks) can be generated by the diagenesis of previous weathering products, resulting in soils derived from sedimentary rocks being systems with "primary CSFs input" (Solleiro-Rebolledo et al., 2023). The lack of data regarding REEs in CSFs of parent materials may lead to insufficient understanding of REE geochemical signals during weathering. Therefore, a comparative study of REEs in CSFs between parent materials and soils, particularly saprolites, is necessary to optimize the existing weathering model of sedimentary rock crust. This approach would also allow for a re-evaluation of the reliability of REEs as a fingerprint for tracing regional surface processes.

Deciphering geochemical signals in REEs within CSFs requires constraining the actual REE content and pattern for each phase. Chemical extraction is typically employed for quantitatively characterizing and isolating individual mineral phases (Land et al., 1999; Laveuf et al., 2012; Fu et al., 2019; Liu et al., 2023; Denys et al., 2021; Durn et al., 2021; Wu et al., 2022). Recent research by Wu et al. (2022) quantified the CBD (citrate-bicarbonate-dithionite)-extractable REEs, which may account for approximately 60 % of the total REE content in soils derived from four types of silicate rock. They identified an interesting phenomenon: the CBD-extractable fractions displayed an enrichment of LREEs, which contradicts the association preference between HREEs and iron oxides (Wu et al., 2022). One possible explanation for this disagreement is the lack of distinction between amorphous iron oxides (Fe_{ox1}) and crystalline iron oxides (Fe_{ox2}), which usually have different REE contents and patterns (Koeppenkastrop and Carlo, 1992; Jiang et al., 2011; Liu et al., 2023). To obtain quantitative information about the relationship between REEs and clay-sized minerals, we employed the sequential extraction procedure of Lu et al. (2017) in this work, which has been used to distinguish REE speciation in CSFs (Liu et al., 2023). Additionally, considering the possibility of clay-sized phases scavenging REEs from the liquid phase (Bradbury and Baeyens, 2005; Stille et al., 2009; Liu et al., 2022), we obtained a soil water sample to explain REE fractionation in the clay-sized mineral phases.

This study systematically investigated REE speciation of CSFs of saprolites and their parent materials (including carbonate and clastic rocks) across a regional scale, leveraging the natural gradient of different lithologies in the Chongqing region of southwest China. The objectives of this study were to: (1) determine the REE content and speciation in CSFs of different sedimentary rocks and their saprolites; (2) clarify the distribution and redistribution of REEs among clay-sized phases during the weathering process; and (3) reveal the geochemical implications of REE fractionation in clay-sized mineral phases.

2. Materials and methods

2.1. Study area and sample collection

The study area was located in Chongqing (105° 11′–110° 11′ E, 28° 10′–32° 13′ N), southwest China, where sedimentary rocks are widely distributed, accounting for more than 95 % of the area. As a component of the karstic region of southwest China, the study area is characterized by the alternating outcrop of carbonate strata (predominantly Triassic, Ordovician, and Cambrian) and clastic rock strata (mainly Cretaceous, Jurassic, Permian, and Silurian) (Fig. 1). Thin and non-uniform soils (10–100 cm) have developed and cover the mountainous topography, enabling convenient investigation of REE behavior during the incipient

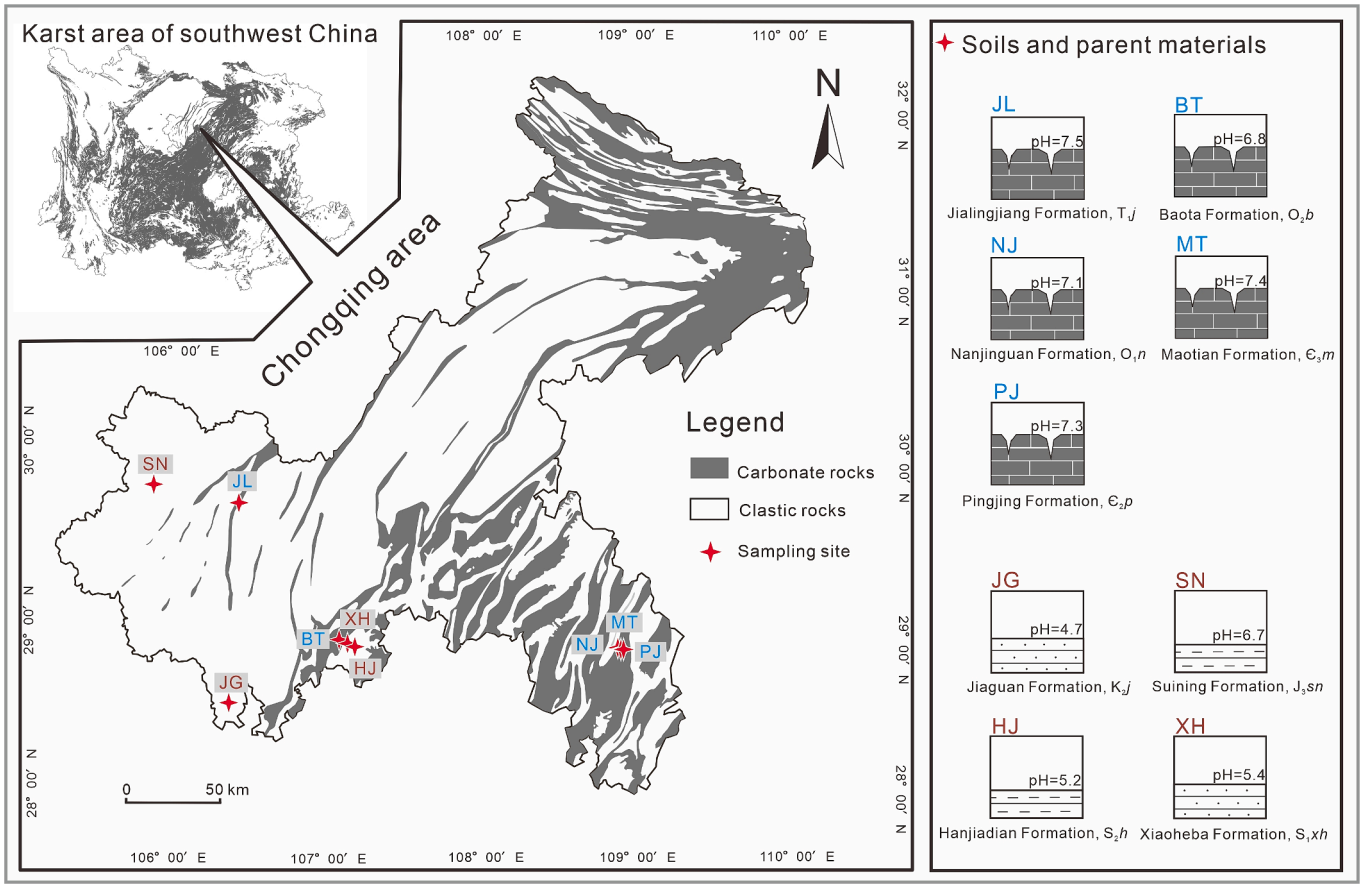

Fig. 1. Location and layout of sampling sites (modified from Zeng et al., 2016).

weathering of different sedimentary rocks. According to regional investigations by Zhang et al. (2023) and Yu et al. (2023), the majority of local soils correspond to Luvisols in the World Reference Base for Soil Resources (WRB) system (IUSS Working Group WRB, 2015).

In the study area, the collected samples included five limestones from the Triassic Jialingjiang (JL) Formation, Ordovician Baota Formation (BT), Cambrian Nanjinguan (NJ) Formation, Cambrian Mentian (MT) Formation, and Cambrian Pinjing (PJ) Formation; two sandstones from the Cretaceous Jiaguan (JG) Formation and Silurian Xiaoheba (XH) Formation; and two shales from the Jurassic Suining (SN) Formation and Silurian Hanjiadian (HJ) Formation. Additionally, a total of nine saprolites (soil layer 5 cm directly above the rock surface) were collected (Fig. 1). Rock samples are noted by the abbreviation of the sampling site + R, e.g., JLR; while soil samples are noted by the abbreviation of the sampling site + S, e.g., JLS. All sampling sites were chosen from mountaintops or slopes with the same lithology, avoiding the slope foot. Considering the similar phyllosilicate composition between saprolites and parent materials (Fig. S1), there could be little input from allochthonous materials to the sampling sites. Moreover, limited anthropogenic disturbances were identified around the sampling sites. The local soils had approximately 30 % clay content (Hu et al., 2023; Yu et al., 2023). Saprolites derived from carbonate rocks possessed neutral to alkaline pH (6.8–7.5, both with soil weight to solution volume, w/v = 1:2.5), while saprolites from clastic rocks had neutral to acidic pH (4.7–6.7) (Fig. 1).

A simple soil water collection device was inserted into the layer 5 cm above the rock surface at the JL sampling site to obtain a soil water sample (gravitational water). The device consisted of a polyethylene tray, a polyethylene bottle, and a tube, as depicted in Fig. S2. The collected soil water was filtered through a 0.22 μm membrane and immediately stabilized following collection using HNO_3 (2 % v/v).

2.2. Separation of clay-sized fractions

The CSFs were separated from bulk samples through centrifugation in deionized water according to Stokes law (Ji et al., 1999). For carbonate rocks, the CSFs were separated from the "hydrochloric acid (HCl) insoluble matter", which was treated by acid leaching with 1 M HCl to remove the carbonate component (Wang et al., 1999; Ji et al., 2004; Yang et al., 2021). A recent report indicates that there might be partial dissolution of non-carbonate phases due to the above treatment (< 4%) (Asgar et al., 2023). However, the limited content of Si (< 2.5 mg kg^{-1}) and Al (< 17.6 mg kg^{-1}) in the HCl-extractable fractions from representative carbonate rocks (i.e., JLR, BTR, and NJR, Table S1) suggests that the limited dissolution of non-carbonate phases would scarcely influence the issues of concern in this work. For clastic rocks, the CSFs were separated from broken rocks after soaking in deionized water for 24 h. After separation, the content of resistant REE-bearing minerals (e.g., apatite, monazite, zircon) was decreased, given their greater specific gravity (> 3 g cm^{-3}) compared to CSFs (typically < 2.7 g cm^{-3}), which could cause preferential settling.

2.3. X-ray diffraction analysis

Oriented CSFs were examined using a Bruker D8 Advance diffractometer with Cu-Kα radiation under dry air conditions at a voltage of 40 kV and a current of 40 mA. The oriented sections were scanned with a goniometer from 3° to 50° 2θ, with a step size of 0.01°. The relative abundance of individual phyllosilicates was estimated from the XRD powder diagrams. Semi-quantitative calculations of illite (10 Å) and chlorite + kaolinite (7 Å) were performed using MDI JADE 6 software (peak height), with corresponding intensification factors of 4 and 2 for illite and chlorite + kaolinite, respectively. The relative levels of chlorite and kaolinite were distinguished by the intensity of their respective peaks at 3.53 Å and 3.56 to 3.58 Å (Cook et al., 1975). The deviation of this method was estimated to be about 8–10 % of the relative abundance of individual phyllosilicates.

2.4. Sequential extraction procedure

The sequential extraction procedure followed the method of Lu et al. (2017). The sequence of the extraction procedure was as follows:

In Step 1 (organic matter), 100 mg of dried CSFs were treated with 2 mL of 30 % hydrogen peroxide to dissolve organic matter. Following intensive mixing, the mixture was reacted for 12 h.

In Step 2 (amorphous iron oxides, Fe_{ox1}), 50 mL of extraction agent (1 M hydroxylamine hydrochloride and 25 % (v/v) acetic acid) was added to the residue from Step 1. After shaking three times for 10 min every 30 min, the sample was reacted in dark conditions for 24 h to dissolve amorphous iron oxide (hydroiron).

In Step 3 (crystalline iron oxides, Fe_{ox2}), the CBD (citrate-bicarbonate-dithionite) procedure was employed to dissolve the reducible iron oxides (generally referred to as free iron). The residue of Step 2 was treated with 45 mL of 0.3 M citrate, 5 mL of 1 M bicarbonate solution, and excess dithionite powder and shaken for 30 min at 80 °C.

In Step 4 (phyllosilicates), boiling HCl was utilized to dissolve iron-containing phyllosilicate minerals, such as chlorite, nontronite, glauconite, and biotite. The residue of Step 3 was boiled with 3 mL of 6 M HCl for 2 h, and the volume was adjusted to 50 mL.

In Step 5 (residue), HCl, HNO_3, and hydrofluoric acid were added to the residue of Step 4 in a Teflon beaker and repeatedly digested at 210 °C to dissolve the refractory fractions. After each extraction step, samples were centrifuged for 15 min at a speed of 5,000 r min^{-1}, and the volume of liquids was adjusted to 50 mL using a 2 % HNO_3 solution.

2.5. Chemical analysis

Chemical analyses were conducted at Guizhou Tongwei Analytical Technology Co., Ltd., using ICP-MS (Thermo, ICP-MS X2, USA). The ICP-MS procedure for REE analysis followed the protocol by Eggins et al. (1997) and was modified by the Radiogenic Isotope Laboratory (Kamber et al., 2003; Lawrence et al., 2006). USGS W2a was used as the reference standard and cross-checked with BIR-1, BHVO-2, and JCp-1 standards. Instrument drift and mass bias were corrected using internal standards and external monitors. The precision of detection was better than 2 %.

3. Results and discussion

3.1. REE speciation in CSFs of parent materials

CSFs of parent materials could be one of the initial REE carriers for soils (Solleiro-Rebolledo et al., 2023). In our study, the total REE content in CSFs of different parent materials ranged from 41.2 to 144.6 mg kg^{-1} (Fig. 2a and b), which is comparable to the values reported by Cullers et al. (1979) for Permian platform sedimentary rocks, suggesting a normal level of REE abundance in CSFs of sedimentary rocks.

Although the analyzed CSFs from different strata had varying total REE contents (Fig. 2a and b), potentially governed by their individual sedimentary facies (Cullers et al., 1979), the REE speciation of major CSFs was similar, except for the sample XHR. The proportion of each REE speciation generally followed: Fe_{ox1} (average = 56.4 %, n = 9, SD = 14.3 %) > Fe_{ox2} (average = 24.1 %, n = 9, SD = 7.9 %) > phyllosilicates (average = 17.5 %, n = 9, SD = 9.5 %) > residue (average = 1.3 %, n = 9, SD = 1.7 %) > organic matter (average = 0.5 %, n = 9, SD = 0.1 %) (Fig. 2a and b). This REE distributions among clay-sized phases revealed that over 95 % of the REE abundance in CSFs was constrained mainly by Fe_{ox1}, followed by Fe_{ox2} and phyllosilicates.

The Fe_{ox1} of REE in parent materials ranged from 12.2 to 102.5 mg kg^{-1} (Fig. 2a and b), accounting for over half of the total REEs in CSFs. In previous research regarding carbonate-marl-shale succession, a correlation between REEs and Fe was found (Worash and Valera, 2002). In this study, our data suggest that Fe_{ox1} could be the main host for REEs in

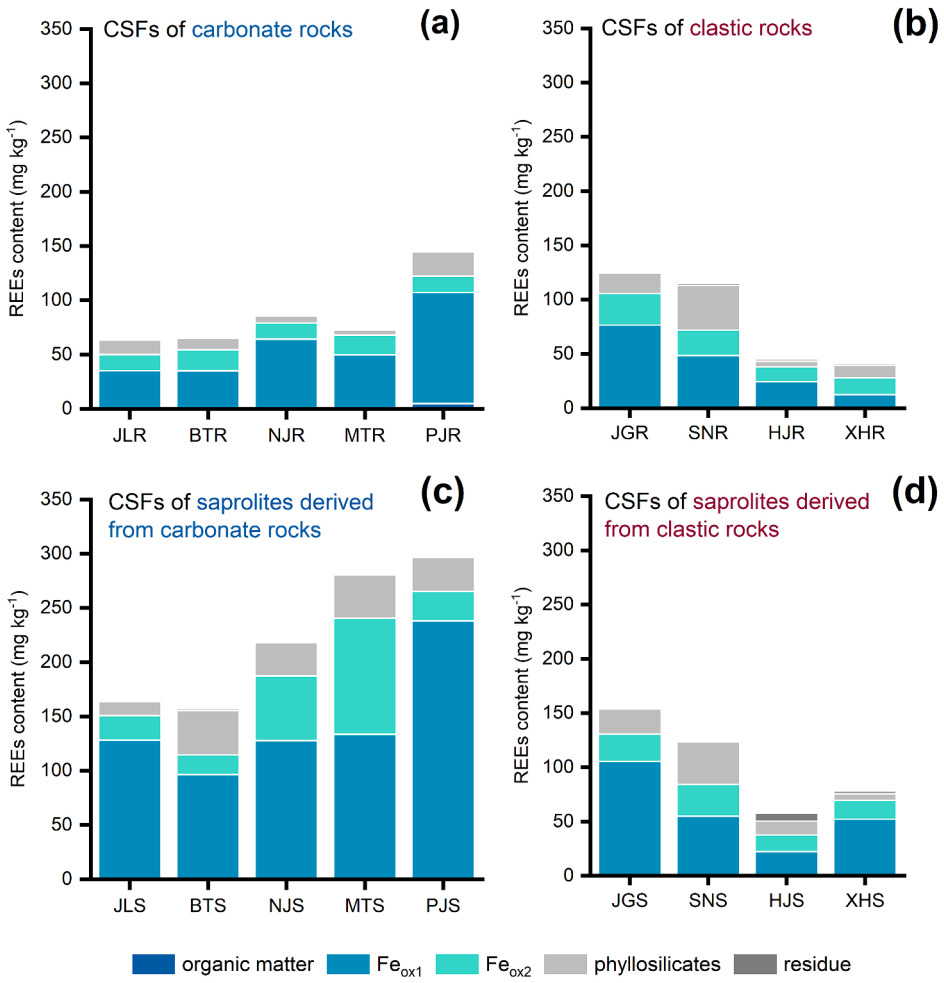

Fig. 2. REE contents and speciation in CSFs of carbonate rocks (a), clastic rocks (b), saprolites derived from carbonate rocks (c), and saprolites derived from clastic rocks (d). The operationally defined fractions of REEs in organic matter, Feo_{x1}, Fe_{ox2}, phyllosilicates and residue were acquired from sequential extraction.

CSFs of sedimentary rocks. This observation is supported by several laboratory studies, which indicate that the incorporation of REEs into the iron oxide structure can trigger defects in the crystal lattice (Dardenne et al., 2002), resulting in high REE content in the Fe_{ox1} (Yang et al., 2021).

In comparison, the CBD-extractable fractions (Fe_{ox2}) had lower REEs content (14.8–29 mg kg^{-1}) than Fe_{ox1} (Fig. 2a and b), further supporting the reduced correlation of Fe_{ox2} with REE content relative to Fe_{ox1} in the study by Santos et al. (2019). Throughout the aging and crystallization processes, which encompass a structural change (Raiswell and Canfield, 2012), iron oxides typically expel REEs (Koeppenkastrop and Carlo, 1993), suggesting that Fe_{ox2} could be a minor host for REEs in CSFs of sedimentary rocks.

As for phyllosilicates, our data indicate the REE contents of HCl-extractable fractions (4.9–40.9 mg kg^{-1}, Fig. 2a and b) could be equivalent to those of Fe_{ox2}. Based on XRD analytical results (Fig. S1), the main phyllosilicates in CSFs are illite, chlorite, and sometimes kaolinite. Chlorite, as a prevalent iron-bearing phyllosilicate in CSFs of parent materials, is regarded as a REE-rich carrier (Cullers et al., 1975; Laveuf and Cornu, 2009). Theoretically, the REE enrichment potentially arises from the crystal structure of chlorite and may enable broad isomorphic substitution in the octahedrally-coordinated layers (such as Fe or Al, Worden et al., 2020).

3.2. REE accumulation enhanced during carbonate rock weathering

Soils generated from sedimentary rocks could be regarded as systems with "primary clay-sized minerals input" (Solleiro-Rebolledo et al., 2023). As illustrated in Fig. 2c and d, the CSFs of saprolites had REE contents ranging from 57.8 to 297.2 mg kg^{-1}, approximately 108.7 % to 384.9 % of those in corresponding parent materials, suggesting that REEs accumulated in CSFs during the weathering of sedimentary rocks. In comparison, the REE content of CSFs in JLS, BTS, NJS, MTS, and PJS (164.6–297.2 mg kg^{-1}, Fig. 2c) was 2.0 to 3.8 times higher than that in their respective parent materials, which is greater than the elevated levels during weathering of clastic rocks (1.1 to 1.9 times, Fig. 2d). This emphasizes that REE accumulation in CSFs could be linked to the weathering of different lithologies, which is particularly enhanced during the weathering of carbonate rocks.

From the perspective of speciation, Fe_{ox1}, as the major REE-bearing phase in saprolites from carbonate rocks, had an REE content of 95.6–237.5 mg kg^{-1} (Fig. 2c), approximately triple that of parent materials. This suggests that Fe_{ox1} is the hyperaccumulator for REEs in saprolites derived from carbonate rocks. As illustrated by a recent laboratory study, there are approximately 2 times more REEs incorporated in ferrihydrite at pH 7 than at pH 5 (Yang et al., 2021). Generally, the decarbonation process could inhibit the increase of soil acidity during the pedogenesis of carbonate rocks (Ulrich, 1986; Liu et al., 2013). Saprolites derived from carbonate rocks had pH values > 7.1 (Fig. 1). In this environment, the deprotonation of Fe-OH groups may allow Fe_{ox1} to capture and contain abundant REE^{3+} (Quinn et al., 2006; Cornell and Schwertmann, 2003), increasing the REE content in Fe_{ox1}.

Most CSFs in saprolites derived from carbonate rocks had elevated CBD-extractable REE content (17.9–107.1 mg kg^{-1}) compared to parent

materials (14.7–19.4 mg kg^{-1}) (Fig. 2c). As reported by some investigations, the content of CBD-extractable REEs may be related to the abundance of crystalline iron oxides (Chang et al., 2016; Wu et al., 2022). The CBD-extractable Fe content in CSFs of saprolites derived from carbonate rocks has increased approximately 1.7 times compared to that in parent materials (Fig. S3). This result aligns with experimental studies performed by Lewis and Schwertmann (1980), indicating that under neutral to alkaline conditions, ferrihydrite can rapidly transform into crystalline Fe oxides, which could provide more hosts for REEs.

Additionally, Fig. 2c illustrates that HCl-extractable fractions of saprolites derived from carbonate rocks also had higher REE content (13.2–41.2 mg kg^{-1}) than corresponding parent materials (4.9–22.5 mg kg^{-1}). Considering chlorite as a phyllosilicate with limited resistance to weathering (Jackson et al., 1948; Worden et al., 2020; Liao et al., 2023), we speculate that this increase in REE content is possibly related to the partial dissolution/hydrolysis of chlorite during the weathering process of carbonate rocks (Critelli et al., 2014; Liao et al., 2023). Following weathering, REE^{3+} may be more easily incorporated into the weathered chlorite (Michalkova et al., 2005; Liu et al., 2022).

These data offer speciation evidence indicating CSFs are residual REE-bearing components during weathering, as speculated in previous studies regarding bulk karstic soils (Ji et al.,2004; Wei et al., 2014; Feitosa et al., 2020). Critically, this study documents CSFs as sinks for REEs during weathering of carbonate rocks.

3.3. The fingerprint of carbonate rocks weathering

In Fig. 3, the La_N/Yb_N values of CSFs in saprolites were compared to those in their parent materials to decipher the fractionation between LREEs and HREEs in CSFs during weathering. After normalization to post-Archean Australian shale (PAAS, Nance and Taylor, 1976), all samples of complete CSFs displayed HREE enrichment ($La_N/Yb_N < 1$, Fig. 3a), suggesting that CSFs could act as a reservoir for HREEs during sedimentary rock weathering. Moreover, the locations of CSFs of carbonate rocks and their saprolites deviated from the 1:1 line and were near the Y-axis in Fig. 3a, in contrast to the locations of CSFs of clastic rocks and their saprolites, which were distributed along the 1:1 line (Fig. 3a). This suggests that the HREE-enriched fingerprint of CSFs has been weakened during the weathering of carbonate rocks.

To account for this REE fractionation during the weathering of carbonate rocks, REE patterns in mineral phases were quantified to distinguish their specific roles in the REE fractionation of the whole CSFs (Fig. 3). As the primary REE speciation in CSFs, the La_N/Yb_N values of Fe_{ox1} in carbonate rocks and their saprolites were less than 1 and greater than 1, respectively (Fig. 3b). This reflects the enrichment of LREEs over HREEs in Fe_{ox1} during weathering. This observation may be associated with the scavenging of REEs by Fe_{ox1}. Generally, the dissolution of primary REE-bearing minerals contributes to the major REE pool in the soil water (Cidu et al., 2013), and then Fe_{ox1} can scavenge REEs from soil water (Stille et al., 2009). The collected soil water displays an HREE-enriched pattern that mirrors those of REEs in Fe_{ox1} in saprolites from

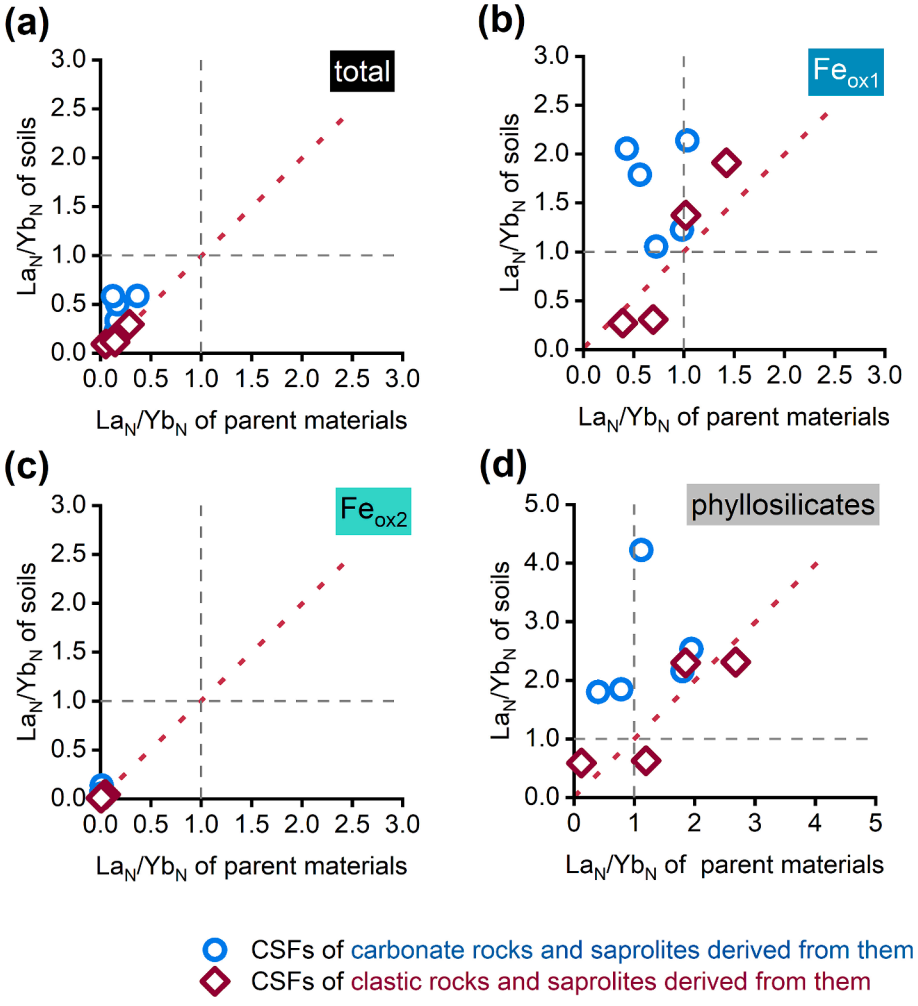

Fig. 3. Plots of La_N/Yb_N of saprolites and parent materials for total CSFs (a) and major clay-sized mineral phases (b)-(d). The N refers to PAAS values from Nance and Taylor (1976).

carbonate rocks (i.e., JLS, Fig. 4). Given that HREEs could combine more easily than LREEs with some ligands in solution, as outlined by prior studies (Koeppenkastrop and Carlo, 1993; Ohta and Kawabe, 2000; Fernández-Caliani et al., 2009), the formation of HREE-Fe_{ox1} associations might be impeded, resulting in a relative deficit of HREEs in Fe_{ox1}.

All locations of the CBD-extractable fractions were concentrated in the bottom left corners, indicating that Fe_{ox2} was characterized by significant HREE enrichment ($La_N/Yb_N < 0.1$) in both saprolites and parent materials (Fig. 3c). This result is in agreement with the CBD-extractable fractions of soils developed from other types of parent materials, such as schist, andesite, and mafic rocks (Wu et al., 2022). This implies that Fe_{ox2} could generally be an HREE-rich mineral phase in the surface environment. During the aging process, due to the greater ionic radii and lower electronegativity, LREEs might be preferentially removed from Fe-oxyhydroxide over HREEs in the same trivalent state (Laveuf and Cornu, 2009).

For phyllosilicates, the La_N/Yb_N values of saprolites from carbonate rocks were also higher than those of their respective parent materials, indicating that more LREEs than HREEs were accumulated in phyllosilicates as weathering proceeds (Fig. 3d). This could be linked to the interaction between phyllosilicates and soil water, potentially resulting in more LREEs being scavenged by phyllosilicates over HREEs (Fig. 4). Additionally, the type and combination of phyllosilicates may also influence this process (Egashira et al., 2004; Laveuf and Cornu, 2009; Andrade et al., 2022). As reported in some studies, chlorite could be HREE-enriched (Cullers et al., 1975). Variation in the relative content of phyllosilicates (Fig. S1) may further increase LREE accumulation over HREEs during carbonate rock weathering.

From the above discussion, it can be inferred that carbonate rock weathering might alter the original REE pattern in clay-sized phases, particularly in Fe_{ox1} and phyllosilicates. REEs in CSFs of karstic soils might record the weathering of carbonate rocks rather than provenances.

4. Conclusions

Clay-sized fractions (CSFs) were REE-bearing carriers from sedimentary rocks to saprolites, with Fe_{ox1} acting as the primary host for REEs. The substantial REE accumulation in clay-sized phases of saprolites directly validated that CSFs were REE sinks during the weathering of carbonate rocks. Additionally, based on analyses of REE patterns, the REE geochemical signals in CSFs likely imply provenance for saprolites developed from clastic rocks (provenance control) rather than weathering signals for saprolites from carbonate rocks (weathering control). Therefore, it is necessary to carefully employ REEs as a fingerprint for tracing material sources, particularly in karst areas, since the original REE signals in CSFs could be modified during the incipient weathering period of karstic soils.

CRediT authorship contribution statement

Xianming Zhang: Writing – review & editing, Writing – original draft, Visualization, Validation, Methodology, Investigation, Formal analysis, Data curation, Conceptualization. **Yuntao Jing:** Writing – review & editing, Supervision, Methodology, Investigation, Formal analysis, Conceptualization. **Wanfu Zhao:** Validation, Supervision, Resources, Investigation, Funding acquisition. **Yongjun Jiang:** Supervision, Resources, Investigation. **Dong-Xing Guan:** Supervision, Validation, Writing – review & editing. **Hongxia Du:** Conceptualization, Supervision, Validation, Writing – review & editing. **Ying Qian:** Writing – review & editing. **Fei Ye:** Validation, Supervision, Resources, Investigation, Funding acquisition, Conceptualization. **Wancang Zhao:** Writing – review & editing, Visualization, Validation, Supervision, Resources, Project administration, Methodology, Funding acquisition, Conceptualization.

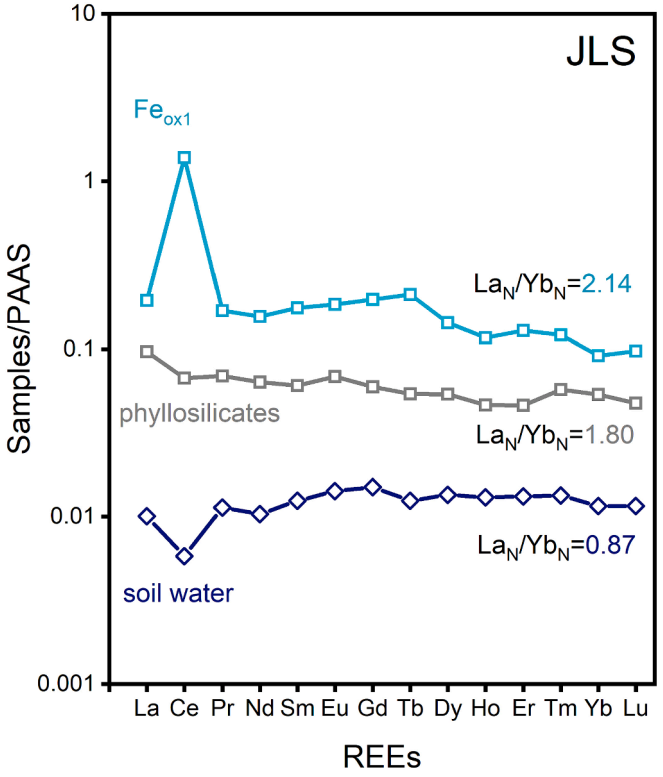

Fig. 4. PAAS-normalized REE patterns for soil water, Fe_{ox1} and phyllosilicates in JLS.

Declaration of competing interest

The authors declare that they have no known competing financial interests or personal relationships that could have appeared to influence the work reported in this paper.

Data availability

Data will be made available on request.

Acknowledgments

This research was funded by the National Natural Science Foundation of China (92162216 and 41673095), and Key Research and Development Project of the Ningxia Hui Autonomous Region, China (2022BEG03054). We thank Shu'e Luo, Tongru Lv, Yixuan Li, Mengni Li, Yurui Cheng, Jiabin Li, Xing Yan, Ke Jiang, Xiaoyong Long and Ran Huang, for their help in the field work, as well as Yuchuan Sun, Hai Wu, Chuan Liu and Jinjiang Pan for their help in performing the experiments. Alberto Agnelli and two anonymous reviewers are acknowledged for providing detailed reviews, which improved our manuscript substantially.

Appendix A. Supplementary data

Supplementary data to this article can be found online at https://doi.org/10.1016/j.geoderma.2024.116879.

References

Andrade, G., Cuadros, J., Barbosa, J., Vidal-Torrado, P., 2022. Clay minerals control rare earth elements (REE) fractionation in Brazilian mangrove soils. Catena 209, 105855. https://doi.org/10.1016/j.catena.2021.105855.

Asgar, H., Mohammed, S., Socianu, A., Kaszuba, J., Shevchenko, P., Gadikota, G., 2023. Dissolution and reprecipitation of amorphous silica in silica Rich shales induces Non-

Monotonic evolution of porosity in acidic reactive environments. Fuel 337, 127144. https://doi.org/10.1016/j.fuel.2022.127144.
Bau, M., Koschinsky, A., 2009. Oxidative scavenging of cerium on hydrous Fe oxide: Evidence from the distribution of rare earth elements and yttrium between Fe oxides and Mn oxides in hydrogenetic ferromanganese crusts. Geochem. J. 43, 37–47. https://doi.org/10.2343/geochemj.1.0005.
Bayon, G., Toucanne, S., Skonieczny, C., André, L., Bermell, S., Cheron, S., Dennielou, B., Etoubleau, J., Freslon, N., Gauchery, T., Germain, Y., Jorry, S., Ménot, G., Monin, L., Ponzevera, E., Rouget, M., Tachikawa, K., Barrat, J., 2015. Rare earth elements and neodymium isotopes in world river sediments revisited. Geochim. Cosmochim. Acta 170, 17–38. https://doi.org/10.1016/j.gca.2015.08.001.
Bradbury, M., Baeyens, B., 2005. Experimental measurements and modeling of sorption competition on montmorillonite. Geochim. Cosmochim. Acta 69, 4187–4197. https://doi.org/10.1016/j.gca.2005.04.014.
Braun, J., Pagel, M., Herbilln, A., Rosin, C., 1993. Mobilization and redistribution of REEs and thorium in a syenitic lateritic profile: a mass balance study. Geochim. Cosmochim. Acta 57, 4419–4434. https://doi.org/10.1016/0016-7037(93)90492-F.
Brioschi, L., Steinmann, M., Lucot, E., Pierret, M., Stille, P., Prunier, J., Badot, P., 2013. Transfer of rare earth elements (REE) from natural soil to plant systems: implications for the environmental availability of anthropogenic REE. Plant Soil 366, 143–163. https://doi.org/10.1007/s11104-012-1407-0.
Cao, X., Chen, Y., Wang, X., Deng, X., 2001. Effects of redox potential and pH value on the release of rare earth elements from soil. Chemosphere 44, 655–661. https://doi.org/10.1016/S0045-6535(00)00492-6.
Chakhmouradian, A., Wall, F., 2012. Rare earth elements: minerals, mines, magnets (and more). Elements 8, 333–340. https://doi.org/10.2113/gselements.8.5.333.
Chang, C., Li, F., Liu, C., Gao, J., Tong, H., Chen, M., 2016. Fractionation characteristics of rare earth elements (REEs) linked with secondary Fe, Mn, and Al minerals in soils. Acta Geochimica 35 (4), 329–339. https://doi.org/10.1007/s11631-016-0119-1.
Chang, C., Song, C., Beckford, H., Wang, S., Ji, H., 2019. Behaviors of REEs during pedogenetic processes in the karst areas of Southwest China. J. Asian Earth Sci. 185, 104023 https://doi.org/10.1016/j.jseaes.2019.104023.
Cidu, R., Antisari, L., Biddau, R., Buscaroli, A., Carobone, S., Pelo, S., Dinelli, E., Vianello, G., Zannoni, D., 2013. Dynamics of rare earth elements in water–soil systems: the case study of the Pineta San Vitale (Ravenna, Italy). Geoderma 193–194, 52–67. https://doi.org/10.1016/j.geoderma.2012.10.009.
Cook, H., Johnson, P., Matti, J., Zemmels, I., 1975. IV. Methods of Sample Preparation, and X-Ray Diffraction Data Analysis, X-Ray Mineralogy Laboratory, Deep Sea Drilling Project. University of California, Riverside. Initial reports of the deep sea drilling project 25.
Cornell, R., Schwertmann, U., 2003. The iron Oxides: Structure, Properties, Reactions, Occurrences and Uses. Wiley-VCH Verlag GmbH & Co, KGaA, Weinheim, p. 661.
Critelli, T., Marini, L., Schott, J., Mavromatis, V., Apollaro, C., Rinder, T., Rosa, R., Oelkers, E., 2014. Dissolution rates of actinolite and chlorite from a whole-rock experimental study of metabasalt dissolution from $2 \leq pH \leq 12$ at 25 °C. Chem. Geol. 390, 100–108. https://doi.org/10.1016/j.chemgeo.2014.10.013.
Cullers, R., Chaudhuri, S., Arnold, B., Lee, M., Wolf, C., 1975. Rare earth distributions in clay minerals and in the clay-sized fraction of the Lower Permian Havensville and Eskridge shales of Kansas and Oklahoma. Geochim. Cosmochim. Acta 39, 1691–1703. https://doi.org/10.1016/0016-7037(75)90090-3.
Cullers, R., Chaudhuri, S., Kilbane, N., Koch, R., 1979. Rare-earths in size fractions and sedimentary rocks of Pennsylvanian-Permian age from the mid-continent of the U.S. A. Geochim. Cosmochim. Acta 43, 1285–1301. https://doi.org/10.1016/0016-7037(79)90119-4.
Dardenne, K., Schafer, T., Lindqvist-reis, P., Denecke, M.A., Plaschke, M., Rothe, J., Kim, J.I., 2002. Low temperature XAFS investigation on the lutetium binding changes during the 2-line ferrihydrite alteration process. Environ. Sci. Technol. 36, 5092–5099. https://doi.org/10.1021/es025513f.
Denys, A., Janots, E., Auzende, A., Lanson, M., Findling, N., Trcera, N., 2021. Evaluation of selectivity of sequential extraction procedure applied to REE speciation in laterite. Chem. Geol. 599, 119954 https://doi.org/10.1016/j.chemgeo.2020.119954.
Durn, G., Perković, I., Stummeyer, J., Ottner, F., Mileusnić, M., 2021. Differences in the behaviour of trace and rare-earth elements in oxidizing and reducing soil environments: Case study of Terra Rossa soils and Cretaceous palaeosols from the Istrian peninsula. Croatia. Chemosphere 283, 131286. https://doi.org/10.1016/j.chemosphere.2021.131286.
Egashira, K., Aramaki, K., Yoshimasa, M., Takeda, A., Yamasak, S., 2004. Rare earth elements and clay minerals of soils of the floodplains of three major rivers in Bangladesh. Geoderma 120, 7–15. https://doi.org/10.1016/j.geoderma.2003.07.005.
Eggins, S.M., Woodhead, J.D., Kinsley, L.P.J., Mortimer, G.E., Sylvester, P., McCulloch, M.T., Hergt, J.M., Handler, M.R., 1997. A simple method for the precise determination of 40 trace elements in geological samples by ICPMS using enriched isotope internal standardisation. Chem. Geol. 134 (4), 311–326. https://doi.org/10.1016/S0009-2541(96)00100-3.
Feitosa, M., Silva, Y., Biondi, C., Alcantara, V., Nascimento, C., 2020. Rare Earth elements in rocks and soil profiles of a tropical volcanic archipelago in the Southern Atlantic. Catena 194, 104674. https://doi.org/10.1016/j.catena.2020.104674.
Fernández-Caliani, J., Barba-Brioso, C., Rosa, J., 2009. Mobility and speciation of rare earth elements in acid minesoils and geochemical implications for river waters in the southwestern Iberian margin. Geoderma 149, 292–401. https://doi.org/10.1016/j.geoderma.2009.01.004.
Fu, W., Li, X., Feng, Y., Feng, M., Peng, Z., Yu, H., Lin, H., 2019. Chemical weathering of S-type granite and formation of Rare Earth Element (REE)-rich regolith in South China: Critical control of lithology. Chem. Geol. 520, 33–51. https://doi.org/10.1016/j.chemgeo.2019.05.006.
Gu, Q., Liu, J., Yang, Y., Zhu, R., Ma, L., Liang, X., Long, S., Zhu, J., He, H., 2022. The different effects of sulfate on the adsorption of REEs on kaolinite and ferrihydrite. Appl. Clay Sci. 221, 106468 https://doi.org/10.1016/j.clay.2022.106468.
Hu, J., Huang, Z., Li, S., Liu, B., Ci, E., 2023. Assessing profile uniformity of soils from weathered clastic sedimentary rocks in southwest China. Catena 224, 107007. https://doi.org/10.1016/j.catena.2023.107007.
IUSS Working Group WRB, 2015. World Reference Base for Soil Resources 2006, first update 2007. World Soil Resources Reports No. 103. FAO, Rome.
Jackson, M., Tyler, S., Willis, A., Bourbeau, G., Pennington, R., 1948. Weathering sequence of clay-size minerals in soils and sediments. I. Fundamental generalizations. J. Phys. Chem. 52, 1237–1260. https://doi.org/10.1021/j150463a015.
Ji, J., Chen, J., Lu, H., 1999. Origin of illite in the loess from the Luochuan area, Loess Plateau. Central China. Clay Miner. 34, 525–532. https://doi.org/10.1180/000985599546398.
Ji, H., Wang, S., Ouyang, Z., Zhang, S., Sun, C., Liu, X., Zhou, D., 2004. Geochemistry of red residua underlying dolomites in karst terrains of Yunnan-Guizhou Plateau. Chem. Geol. 203, 29–50. https://doi.org/10.1016/j.chemgeo.2003.08.012.
Jiang, X., Lin, X., Yao, D., Guo, W., 2011. Enrichment mechanisms of rare earth elements in marine hydrogenic ferromanganese crusts. Sci China Earth Sci. 54, 197–203. https://doi.org/10.1007/s11430-010-4070-4.
Kamber, B.S., Greig, A., Schoenberg, R., Collerson, K.D., 2003. A refined solution to Earth's hidden niobium: Implications for evolution of continental crust and mode of core formation. Precambr. Res 126, 289–308. https://doi.org/10.1016/S0301-9268(03)00100-1.
Koeppenkastrop, D., Carlo, E., 1992. Sorption of rare-earth elements from seawater onto synthetic mineral particles: an experimental approach. Chem. Geol. 95, 251–263. https://doi.org/10.1016/0009-2541(92)90015-W.
Koeppenkastrop, D., Carlo, E., 1993. Uptake of rare earth elements from solution by metal oxide. Environ. Sci. Technol. 27, 1796–1802. https://doi.org/10.1021/es00046a006.
Land, M., Ohlander, B., Ingri, J., Thunberg, J., 1999. Solid speciation and fractionation of rare earth elements in a spodosol profile from northern Sweden as revealed by sequential extraction. Chem. Geol. 160, 121–138. https://doi.org/10.1016/S0009-2541(99)00064-9.
Laveuf, C., Cornu, S., 2009. A review on the potentiality of Rare Earth Elements to trace pedogenetic processes. Geoderma 2009 (154), 1–12. https://doi.org/10.1016/j.geoderma.2009.10.002.
Laveuf, C., Cornu, S., Guilherme, L., Guerin, A., Juillot, F., 2012. The impact of redox conditions on the rare earth element signature of redoximorphic features in a soil sequence developed from limestone. Geoderma 170, 25–38. https://doi.org/10.1016/j.geoderma.2011.10.014.
Lawrence, M.G., Greig, A., Collerson, K.D., Kamber, B.S., 2006. Direct quantification of rare earth element concentrations in natural waters by ICP-MS. Applied Geochem. 21, 839–848. https://doi.org/10.1016/j.apgeochem.2006.02.013.
Lewis, D.G., Schwertmann, U., 1980. The effect of [OH] on the goethite produced from ferrihydrite under alkaline conditions. J. Colloid Interface Sci. 78 (2), 543–553. https://doi.org/10.1016/0021-9797(80)90591-3.
Liao, R., Gu, X., Brantley, S., 2023. Weathering of chlorite from grain to watershed: The role and distribution of oxidation reactions in the subsurface. Geochim. Cosmochim. Acta 333, 284–307. https://doi.org/10.1016/j.gca.2022.07.019.
Liu, Y., Jing, Y., Zhao, W., 2023. Distribution of rare earth elements and implication for Ce anomalies in the clay-sized minerals of deep-sea sediment. Western Pacific Ocean. Appl. Clay Sci. 235, 106876 https://doi.org/10.1016/j.clay.2023.106876.
Liu, W., Liu, C., Zhao, Z., Xu, Z., Liang, C., Li, L., Feng, J., 2013. Elemental and strontium isotopic geochemistry of the soil profiles developed on limestone and sandstone in karstic terrain on Yunnan-Guizhou Plateau, China: Implications for chemical weathering and parent materials. J. Asian Earth Sci. 67–68, 138–152. https://doi.org/10.1016/j.jseaes.2013.02.017.
Liu, X., Tournassat, C., Grangeon, S., Kalinchev, A., Takahashi, Y., Fernandes, M., 2022. Molecular-level understanding of metal ion retention in clay-rich materials. Nat. Rev. Earth Environ. 3, 461–476. https://doi.org/10.1038/s43017-022-00301-z.
Lu, W., Zhao, W., Balsam, W., Lu, H., Liu, P., Lu, Z., Ji, J., 2017. Iron mineralogy and speciation in clay-sized fractions of Chinese desert sediments. J. Geophys. Res.: Atmos. 122, 13458–13471. https://doi.org/10.1002/2017JD027733.
Michalkova, A., Johnson, L., Gorb, L., Zhikol, O., Shishkin, O., Leszczynski, J., 2005. Theoretical study of adsorption of methyltert-butyl ether on broken clay minerals surfaces. Int. J. Quantum Chem. 105, 325–340. https://doi.org/10.1002/qua.20708.
Nance, W.B., Taylor, S.R., 1976. Rare earth element patterns and crustal sedimentary rocks. Geochim. Cosmochim. Acta 40, 1539–1551. https://doi.org/10.1016/0016-7037(94)90195-3.
Nesbitt, H., Markovics, G., 1997. Weathering of granodioritic crust, long-term storage of elements in weathering profiles, and petrogenesis of siliciclastic sediments. Geochim. Cosmochim. Acta 61, 1653–1670. https://doi.org/10.1016/S0016-7037(97)00031-8.
Ohta, A., Kawabe, I., 2000. REE (III) adsorption onto Mn dioxide (δ-MnO2 and Fe oxyhydroxide: Ce (III) oxidation by δ-MnO2). Geochim. Cosmochim. Acta 65, 695–703. https://doi.org/10.1016/S0016-7037(00)00578-0.
Quinn, K.A., Byrne, R.H., Schijf, J., 2006. Sorption of yttrium and rare earth elements by amorphous ferric hydroxide: influence of solution complexation with carbonate. Geochim. Cosmochim. Acta 70, 4151–4165. https://doi.org/10.1016/j.gca.2006.06.014.
Raiswell, R., Canfield, D., 2012. The iron biogeochemical cycle past and present. Geochem Perspect 1, 1–220. https://doi.org/10.7185/geochempersp.1.1.
Santos, J., Pera, E., Oliveria, C., Júnior, V., Pedron, F., Corrêa, M., Azevedo, A., 2019. Impact of weathering on REE distribution in soil-saprolite profiles developed on

orthogneisses in Borborema Province, NE Brazil. Geoderma 347, 103–117. https://doi.org/10.1016/j.geoderma.2019.03.040.
Solleiro-Rebolledo, E., García-Ramírez, P., Sedov, S., Cabadas-Báez, H., Uria-Rivera, Y., Ibarra-Arzave, G., Pi-Puig, T., 2023. Interaction of geomorphic processes and long-term human impact in the soil evolution: A study case in the tropical area at Veracruz, Mexico. CATENA 227, 107072. https://doi.org/10.1016/j.catena.2023.107072.
Stille, P., Pierret, M., Steinmann, M., Chabaux, F., Boutin, R., Aubert, D., Pourcelot, L., Morvan, G., 2009. Impact of atmospheric deposition, biogeochemical cycling and water–mineral interaction on REE fractionation in acidic surface soils and soil water (the Strengbach case). Chem. Geol. 264, 173–186. https://doi.org/10.1016/j.chemgeo.2009.03.005.
Ulrich, B., 1986. Natural and anthropogenic components of soil acidification. Z. Pflanzenernaehr. Bodenk. 149, 702–717. https://doi.org/10.1002/jpln.19861490607.
Wang, S., Ji, H., Ouyang, Z., Zhou, D., Zhen, L., Li, T., 1999. Preliminary study on weathering and pedogenesis of carbonate rock. Sci China Earth Sci. 42, 572–581. https://doi.org/10.1007/BF02877784.
Wei, X., Ji, H., Wang, S., Chu, H., Song, C., 2014. The formation of representative lateritic weathering covers in south-central Guangxi (southern China). Catena 118, 55–72. https://doi.org/10.1016/j.catena.2014.01.019.
Worash, G., Valera, R., 2002. Rare earth element geochemistry of the Antalo Supersequence in the Mekele Outlier (Tigray region, northern Ethiopia). Chem. Geol. 182, 395–407. https://doi.org/10.1016/S0009-2541(01)00328-X.
Worden, R.H., Griffiths, J., Wooldridge, L.J., Utley, J.E.P., Lawan, A.Y., Muhammed, D. D., Simon, N., Armitage, P.J., 2020. Chlorite in sandstones. Earth-Sci. Rev. 204, 103105 https://doi.org/10.1016/j.earscirev.2020.103105.
Wu, C., Chu, M., Huang, K., Hseu, Z., 2022. Rare earth elements associated with pedogenic iron oxides in humid and tropical soils from different parent materials. Geoderma 423, 115966. https://doi.org/10.1016/j.geoderma.2022.115966.
Wu, C., Hseu, Z., 2023. Pedochemical behaviors of rare earth elements in soil profiles along a lithosequence in eastern Taiwan. Catena 225, 107047. https://doi.org/10.1016/j.catena.2023.107047.
Wu, K., Liu, S., Kandasamy, S., Jin, A., Lou, Z., Li, J., Wu, B., Wang, X., Mohamed, C., Shi, X., 2019. Grain-size effect on rare earth elements in Pahang River and Kelantan River, Peninsular Malaysia: Implications for sediment provenance in the southern South China Sea. Cont. Shelf Res. 189, 103977 https://doi.org/10.1016/j.csr.2019.103977.
Yang, M., Liang, X., Li, Y., He, H., Zhu, R., Arai, Y., 2021. Ferrihydrite transformation impacted by adsorption and structural incorporation of rare earth elements. ACS Earth Space Chem. 5, 2768–2777. https://doi.org/10.1021/acsearthspacechem.1c00159.
Yu, P., Liu, J., Tang, H., Ci, E., Tang, X., Liu, S., Ding, Z., Ma, M., 2023. The increased soil aggregate stability and aggregate-associated carbon by farmland use change in a karst region of Southwest China. Catena 231, 107284. https://doi.org/10.1016/j.catena.2023.107284.
Zeng, S., Jiang, Y., Liu, Z., 2016. Assessment of climate impacts on the karst-related carbon sink in SWChina using MPD and GIS. Glob. Planet. Change 144, 171–181. https://doi.org/10.1016/j.gloplacha.2016.07.015.
Zhang, W., Wu, W., Li, J., Liu, H., 2023. Climate and topography controls on soil water-stable aggregates at regional scale: Independent and interactive effects. Catena 228, 107170. https://doi.org/10.1016/j.catena.2023.107170.